

# Efficient adsorption of Th(IV) from aqueous solution by modified SBA-15 mesoporous silica

Mutlu Gök<sup>1</sup> · Şenol Sert<sup>1</sup> · Gülçin Özevci<sup>1</sup> · Meral Eral<sup>1</sup>

Received: 17 August 2017/Revised: 25 September 2017/Accepted: 19 October 2017/Published online: 28 May 2018  
© Shanghai Institute of Applied Physics, Chinese Academy of Sciences, Chinese Nuclear Society, Science Press China and Springer Nature Singapore Pte Ltd. 2018

**Abstract** A very effective adsorbent for thorium has been obtained by modification of Santa Barbara Amorphous (SBA-15) using the chelating agent thenoyltrifluoroacetone (TTA). The prepared adsorbent (SBA-15-TTA) was characterized using scanning electron microscopy (SEM), Fourier transform infrared spectroscopy (FT-IR), surface area, porosity, and zeta potential analyses. We investigated the factors affecting Th(IV) adsorption on TTA-SBA-15, such as initial pH, contact time, temperature, and initial metal concentration. The effective initial pH for adsorption was found to be 4. The binding sites on TTA-SBA-15 adsorbent were saturated using an initial Th(IV) concentration of 100 mg L<sup>-1</sup>. The *Dubinín–Radushkevich* isotherm suggested a strong chemical interaction between adsorbent and adsorbate. Contact time and temperature had no significant effect on the adsorption. Therefore, the studies show that TTA-SBA-15 is a promising adsorbent to treat Th(IV)-contaminated effluents.

**Keywords** Thorium · SBA-15 · Adsorption · TTA · Radionuclide

## 1 Introduction

Thorium is a long-lived radionuclide spread throughout the earth's crust in many geological forms such as xenotime, monazite, and bastnasite [1]. It is considered an alternative nuclear fuel to uranium due to its abundance in the earth's crust, chemical stability, high radiation resistance, and low radiotoxic waste production [2]. Mining activities and nuclear industry are the main producers of thorium waste. Due to its radioactive character and heavy metal toxicity, the release of thorium waste is an important issue in terms of both human health and environment. Therefore, the recovery of Th(IV) from aqueous solution is a relevant challenge from an environmental and economic point of view.

The treatment of liquid effluents containing high concentrations of metal ions can be performed using some conventional methods like ion exchange, chemical precipitation, filtration, evaporative recovery, and reverse osmosis. Nevertheless, these methods are expensive and inefficient when the waste metal concentration is up to the 100 mg L<sup>-1</sup> [3]. Adsorption is another technique used for separation and purification in dilute solutions. Many sophisticated synthetic materials have been recently developed for adsorption of radionuclides from aqueous solutions. Metal–organic frameworks (MOFs) are one of the materials that can be used for partitioning and remediation of radioactive contaminants. Wei et al. developed mesoporous luminescent MOFs for detection of uranium in several water samples [4]. The Tc<sup>99</sup> radioisotope, having long half-life, high fission yield, and high mobility, was removed in its anionic form (TcO<sub>4</sub><sup>-</sup>) from contaminated waters by such an MOF [5]. To remove uranyl ions from aqueous solutions, ultrastable zirconium phosphonate was

---

This work was supported by the Scientific Technological Research Council of Turkey (No. 113Y557).

✉ Şenol Sert  
senol.sert@ege.edu.tr

<sup>1</sup> Institute of Nuclear Sciences, Ege University,  
35100 Bornova-Izmir, Turkey

developed. The prepared MOF structure showed high stability in the otherwise harsh chemical conditions [6]. Yanlong et al. investigated the structure of uranyl ions coordinated with polycarbonate compounds and observed that the synthesized material exhibits high chemical and radiation resistance in aqueous solutions. It can be used for the treatment of radioactive solutions containing cesium [7]. Many modified and unmodified sorbents were used for adsorption of Th(IV) from liquid effluents, such as PVA/TiO<sub>2</sub>/ZnO nanofiber adsorbent functionalized with mercapto groups [8], amino-magnetic glycidyl methacrylate resins [2], alumina and silica [9], goethite [10], and TiO<sub>2</sub> [11].

Mesoporous silica structures like MCM-48, MCM-41, HMS, and SBA-15 show suitable adsorbent features due to their narrow pore-size distribution, controlled pore sizes, and large surface area [12]. Additionally, the adsorption affinity toward metal ions can be enhanced by modification of silica structures with suitable functional groups [13]. The well-ordered hexagonal mesoporous silica structure, i. e., SBA-15, was synthesized by Zhao et al. [14]. The SBA-15 silica structure has attracted the attention of many adsorption studies because of its distinctive features. Due to its large and controlled pore diameter (5–30 nm), enabling the diffusion of metal ions into the internal pore structures, fast adsorption kinetics could be easily realized. Furthermore, its thick pore walls (4 nm) enhance mechanic and hydrothermal stability of the structure. These striking properties make SBA-15 a suitable support to many functional groups for use in the adsorption of metal ions [15]. Modified with Schiff base ligands *N*-propylsalicylaldehyde and ethylenediaminepropylsalicylaldehyde, SBA-15 adsorbents were used for the removal of uranium(VI) ions from aqueous solutions, as a function of aqueous-phase pH, contact time, adsorbent dose, initial metal ion concentration, and ionic strength [16]. Wang et al. investigated Pb<sup>2+</sup> adsorption on amino-functionalized core-shell magnetic mesoporous SBA-15 silica composite. They easily removed the adsorbent from solution using external magnetic field and regeneration of the sorbent was achieved by acid treatment [17]. SBA-15 materials functionalized by 3-aminopropyl-triethoxysilane and bis(2,4,4-trimethylpentyl)phosphinic acid (Cyanex 272) were employed for the adsorption of some heavy metal ions from aqueous solution. Remarkable adsorption capacities were obtained for Cu<sup>2+</sup>, Co<sup>2+</sup>, and Zn<sup>2+</sup> ions, and high selectivity was achieved for Zn<sup>2+</sup> compared to other ions [18]. Shahbazi et al. conducted batch and column studies for adsorption of Cu(II), Pb(II), and Cd(II) ions from aqueous solution using polyamidoamine-functionalized SBA-15 (PAMAM-SBA-15). The isotherm models, thermodynamic parameters, and kinetic studies were

investigated in the batch mode. The breakthrough curves were obtained using column tests [19].

Thenoyltrifluoroacetone (TTA) is a type of  $\beta$ -diketone derivative used as a chelating agent for metals. Harvianto et al. studied lithium ion recovery from seawater using the solvent extraction method with thenoyltrifluoroacetone-trioctylphosphine oxide (TTA-TOPO) mixed in kerosene [20]. The extraction of the UO<sub>2</sub><sup>2+</sup> ion was investigated by TTA room temperature ionic liquid systems. The results of this study suggested that the extraction mechanism is dominated by cation exchange at lower pH but changed to the ion-pair extraction method at higher pH [21].

In this study, adsorption of thorium from aqueous solution using TTA-modified SBA-15 was investigated. The modified mesoporous structure was characterized to identify its chemical and physical features. The adsorption process was carried out in batch mode, and the effects on the uptake of metal ions were investigated. Isotherm models were used to understand adsorption behaviors.

## 2 Experimental

### 2.1 Materials and methods

The reagents for the preparation of the TTA-SBA-15 sorbent material, tetraethylorthosilicate (TEOS, 99%), Pluronic<sup>®</sup> P123 (EO<sub>20</sub>PO<sub>70</sub>EO<sub>20</sub>), 3-(triethoxysilyl)propyl isocyanate (TEPIC, 95%), 2-thenoyltrifluoroacetone (TTA, 99%), tetrahydrofuran (THF, 99.9%), and sodium hydride (NaH, 95%) were all purchased from Sigma-Aldrich (Saint Louis, USA). Hydrochloric acid (HCl, 37%), ethanol (C<sub>2</sub>H<sub>6</sub>O, 99.5%), nitric acid (HNO<sub>3</sub>, 65%), sodium hydroxide (NaOH), and thorium nitrate pentahydrate (Th (NO<sub>3</sub>)<sub>4</sub>·5H<sub>2</sub>O) were all supplied by Merck (Darmstadt, Germany). The metal solutions of U, Ca, Fe, and Mg were prepared by dissolving appropriate amounts of their nitrate salts to study the effect of coexisting ions on adsorption experiments (Merck, Darmstadt, Germany) in deionized water (resistivity=18.2 MWcm, TOC level=1–5 ppb, Millipore, Milford, MA, USA).

### 2.2 Synthesis of SBA-15

SBA-15 mesoporous silica structure synthesis was adapted from a previously reported study [14]. The reaction mixture consists of 4 g copolymer/0.041 mol TEOS/0.24 mol HCl/6.67 mol H<sub>2</sub>O. The detailed description is as follows: surface active agent was mixed with 14.22 g of distilled water until it became homogeneous; 57.08 g of 2 M HCl was added to the solution and stirred at 35 °C for 2 h. 4.06 g TEOS was then introduced to the mixture dropwise, and the solution was stirred under the same

condition for 24 h. The milky solution obtained was then kept in a Teflon-lined autoclave at 100 °C for a further 24 h. The resulting material was filtered, washed with distilled ethanol and water, and oven-dried. The fine white powder produced was calcined in air at 550 °C for 6 h at a heating rate of 1 °C min<sup>-1</sup>.

### 2.3 Modification of SBA-15

Synthesized SBA-15 material was modified with TTA using the following reflux system [22, 23]: 1 g TTA was dissolved in 40 mL THF. 0.2 g NaH was added slowly. The solution was stirred for 2 h until a yellowish color was observed. 2.5 g TEPIC was introduced to the solution dropwise for 30 min. Resulting material was refluxed at 45 °C under dry nitrogen for 12 h. Synthesized SBA-15 material was added to the reflux system, and the process allowed to continue for a further 12 h. Modified silica material was filtered, washed with ethanol and then water, and dried at room temperature, resulting in a fine light-yellow powder.

### 2.4 Characterization and analysis

The metal concentrations of solutions were measured by inductively coupled plasma optical emission spectrometer (ICP-OES, PerkinElmer Optimal 2000 DV). Scanning electron microscope (SEM) images were obtained with a JEOL JSM-6060. Fourier transform infrared spectroscopy (FT-IR) spectrums were acquired via a Shimadzu FT-IR-8400 S within the wavelengths 400 and 4000 cm<sup>-1</sup>, inclusive. Surface area and porosity values were obtained from nitrogen physisorption isotherms measured at 77 K with a Micromeritics ASAP 2020 analyzer. Zeta potential was measured by a Malvern Nano ZS zetasizer for characterization of TTA-SBA-15.

### 2.5 Batch adsorption studies

The adsorption behavior of TTA-SBA-15 adsorbent was investigated by batch method with a thermostatically controlled shaker (GFL-1083 model). Experiments were conducted by shaking 0.05 g adsorbent with 25 mL metal solution in an Erlenmeyer flask at 150 rpm. Equilibrium concentration of metals was measured by ICP-OES. The adsorbed amount of metals by TTA-SBA-15 was calculated using the following equation:

$$Q = (C_i - C_e) \frac{V}{m} \quad (1)$$

Metal uptake (mg g<sup>-1</sup>) is indicated by  $Q$ , and equilibrium and initial concentration (mg L<sup>-1</sup>) of metal solutions

are indicated by  $C_e$  and  $C_i$ , respectively.  $V$  is the volume of metal solution (L), and  $m$  is the mass of sorbent (g).

## 3 Results and discussion

### 3.1 Preparation and characterization of adsorbent

We prepared TTA-SBA-15 over two steps: the synthesis of the mesoporous silica (SBA-15) and the post-modification of SBA-15 by the TTA chelating agent. The SBA-15 was synthesized by precipitation of TEOS in acidic media to produce an ordered porous silica structure. The slurry product was kept in a Teflon-lined autoclave for hydrothermal treatment. The calcination process was employed to remove organic content, which yields the pure silica structure. The post-modification procedure of SBA-15 by TTA was carried out using the reflux system under dry nitrogen. The final product was characterized using the aforementioned methods and utilized for adsorption experiments.

The values for surface area and porosity shown in Table 1 are comparable with the literature [24–29]. The surface area of SBA-15 decreased by 70% after modification by TTA. Similar decreases in pore diameter and pore volume values have been reported in the literature. These size changes can be interpreted as the result of grafting organic functional groups into the pore structures of SBA-15. SEM images of SBA-15 and TTA-SBA-15 are shown in Fig. 1. SBA-15 material shows a rope-like morphology with an average size of 1 μm. A wheat-like macrostructure due to the aggregation of particles was observed [14]. After grafting the TTA chelating agent, SBA-15 shows similar particle morphology. It shows the stability of the macrostructure after the modification process. The FT-IR spectra of SBA-15 and TTA-SBA-15 can be seen in Fig. 2. The peak between 3760 and 3060 cm<sup>-1</sup> shows the characteristically broad absorption band related to the physically adsorbed water molecules and stretching of the framework's Si–OH groups. The vibrations attributed to the Si–O–Si bonds can be seen at 1063 cm<sup>-1</sup> (asymmetric stretching), 799 cm<sup>-1</sup> (asymmetric stretching), and 482 cm<sup>-1</sup> (bending). The peaks belonging to the characteristic chemical groups of the TTA molecule at 1686 cm<sup>-1</sup> (C=O) and 2934 cm<sup>-1</sup> (C–H, stretching) can be observed on the FT-IR spectra of TTA-SBA-15, which confirms the grafting of the chelating agent into the silica material. Figure 3 shows that the zeta potential of SBA-15 and TTA-SBA-15 decreased with increasing pH. The zero-point charges of the SBA-15 and TTA-SBA-15 materials were found to be 3.8 and 2.7, respectively. Thus, the decrease in zero-point charge was observed by the modification of SBA-15 with TTA extractant.

**Table 1** The results of surface area and porosity analysis

	BET surface area (m <sup>2</sup> g <sup>-1</sup> )	BJH adsorption average pore diameter (nm)	BJH adsorption average pore volume (cm <sup>3</sup> g <sup>-1</sup> )
SBA-15	760	7.10	0.75
TTA-SBA-15	231	4.00	0.33

## 3.2 Adsorption experiments

### 3.2.1 Effect of initial pH on Th(IV) adsorption

Due to the acidity of metal solutions, which has a significant effect on metal uptake, the adsorption of Th(IV) was investigated as a function of the initial pH. The pH of the metal solution influences the adsorbent surface charge and metal speciation directly. Studies on species of thorium in aqueous solutions show that Th(IV) is the least hydrolyzed ion among the tetra positive ions and is stable at pH 3 or less as an uncomplexed cation [30]. According to Cromières et al., the main species of thorium at pH < 4 are Th<sup>4+</sup> (predominating species, 88%) and Th(OH)<sup>3+</sup> (less than 12%) [31]. Therefore, the initial pH value for experiments on the adsorption of Th(IV) was held between 1 and 4 to avoid precipitation of anionic thorium complexes. The effect of initial pH on metal uptake can be seen in Fig. 4. A significant increase in metal adsorption was observed at pH 4. This observation was also supported with the zeta potential analysis: the protonation of TTA-SBA-15 occurs below the zero-point charge (2.7), making the surface charge positive and creating a repulsion force against the cationic forms of metals. By increasing the pH the surface charge changes to negative and metal ions are adsorbed onto the surface. The competition between metal ions and hydrogen ions for the binding sites of the adsorbent at lower pH leads to a decrease in metal adsorption due to the abundance of hydrogen ions [3, 32]. Due to the concern with the precipitation of Th(IV) at pH 4, a blank experiment was carried out. The experiment was done without adsorbent in identical conditions with previous adsorption experiments at pH 4. The concentration of Th(IV) was measured by ICP-OES, and no evidence of Th(IV) precipitation was found.

### 3.2.2 Effect of initial concentration on Th(IV) adsorption

The effect of the initial concentration of metal on the adsorption process is shown in Fig. 5. The effect of the initial concentration on adsorption can further explain the interaction between metal ions and the active sites of the adsorbent surface. The experiments were performed with initial metal concentrations ranging from 40 to 200 mg L<sup>-1</sup>. The adsorption of Th(IV) increased between 40 and

100 mg L<sup>-1</sup> and then plateaued with initial concentrations above 100 mg L<sup>-1</sup>. This can be explained by the increase in the number of metal ions in higher concentrations competing for the available binding sites on the adsorbent. Due to the limited number of binding sites, once all binding sites are occupied, no more Th(IV) ions can be adsorbed [33].

### 3.2.3 Adsorption isotherms

Isotherm models were used to understand the adsorption capacity of the adsorbent by evaluating the equilibrium data. The *Langmuir*, *Freundlich*, and *Dubinin–Radushkevich (D–R)* isotherm models were employed [34, 35]. According to the *Langmuir* theory, the adsorbent has structurally homogeneous and energetically identical adsorption sites. Adsorption occurs at specific adsorption sites inside the adsorbent, and adsorbates cover the surface of the adsorbent in a monolayer formation [36].

The *Langmuir* equation is

$$\frac{C_e}{Q_e} = \frac{1}{bn_m} + \frac{C_e}{n_m}, \quad (2)$$

where  $C_e$  is the equilibrium concentration (mg L<sup>-1</sup>),  $Q_e$  is the amount adsorbed at equilibrium (mg g<sup>-1</sup>), and  $n_m$  and  $b$  are *Langmuir* constants that describe the monolayer capacity and the energy of adsorption, respectively.

The *Freundlich* isotherm model postulates that the surface of the adsorbent has a heterogeneous structure. The empirical *Freundlich* equation is shown below

$$Q_e = KC_e^{1/n}, \quad (3)$$

Its linearized form is

$$\log Q_e = \log k + \left(\frac{1}{n}\right) \log C_e, \quad (4)$$

$Q_e$  indicates the amount of solute adsorbed per unit mass of adsorbent,  $C_e$  indicates the equilibrium concentration, and  $k$  and  $n$  specify the *Freundlich* constants of a particular adsorption isotherm.

The *D–R* isotherm model can be employed for low concentration ranges. It is suitable for the description of both homogeneous and heterogeneous surfaces. The general expression of this model is:

$$\ln X = \ln X_m - K\varepsilon^2. \quad (5)$$

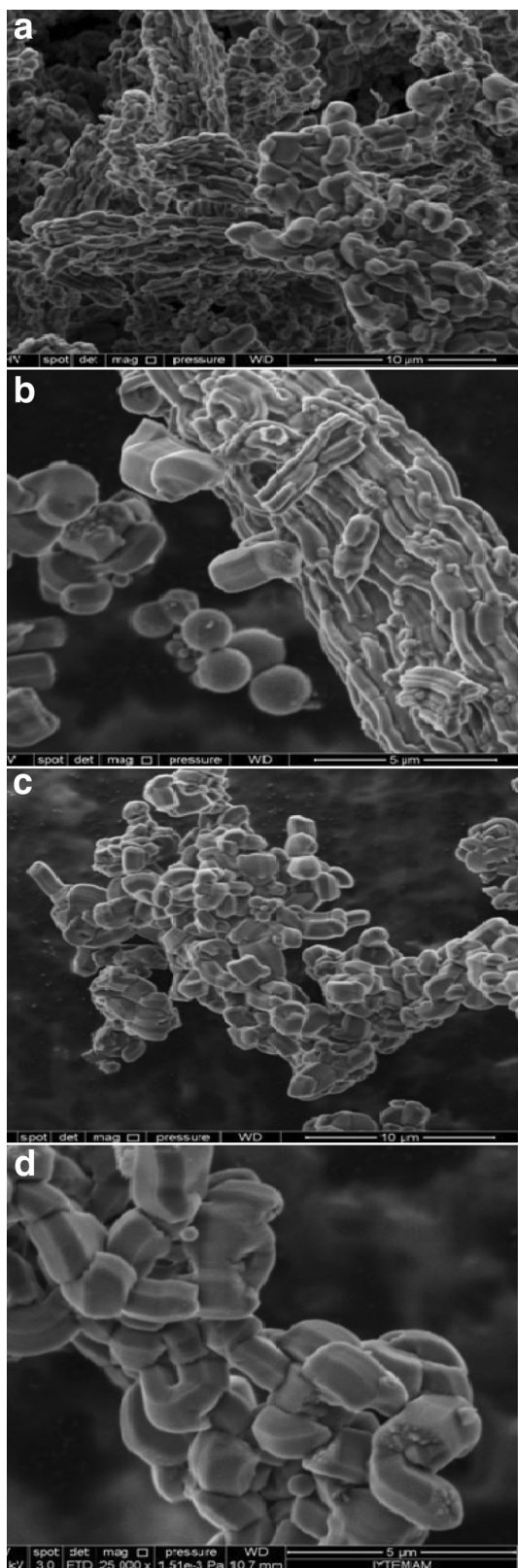


**Fig. 1** SEM images of SBA-15 (a–b) and TTA-SBA-15 (c–d)

$\varepsilon$  is the *Polanyi* potential and is described as follows

$$\varepsilon = RT \ln(1 + 1/C_e). \quad (6)$$

$X$  indicates the mole amount of adsorbate per unit mass of adsorbent,  $X_m$  is the theoretical adsorption capacity, and  $C_e$  is the equilibrium concentration of the adsorbate.  $K$  is the constant associated with the adsorption energy,  $R$  shows the universal gas constant, and  $T$  is the temperature in Kelvin.  $E$  is the average energy of adsorption and is related to the free-energy change when one mol of adsorbate is transferred to the surface of the adsorbent from solution. It is calculated using the equation below

$$E = -(2K)^{-1/2}. \quad (7)$$

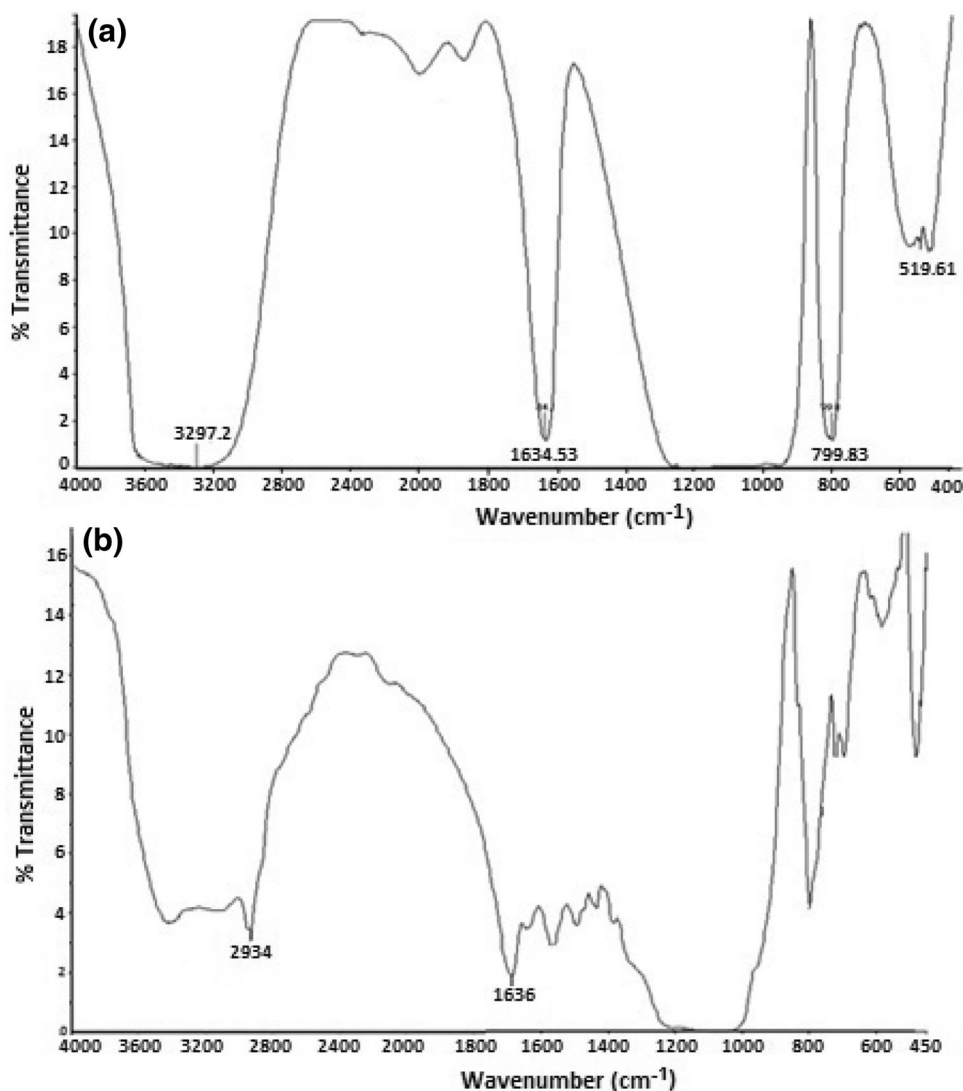
The value of  $E$  can be used to estimate the reaction mechanism. If  $E$  is less than  $8 \text{ kJ mol}^{-1}$ , the physical forces dominate the adsorption mechanism. If the  $E$  values are between  $8$  and  $16 \text{ kJ mol}^{-1}$ , the adsorption is driven by ion exchange. Finally, if  $E$  is greater than  $16 \text{ kJ mol}^{-1}$ , the adsorption is governed by particle diffusion.

The parameters regarding the isotherm models can be seen in Table 2. In terms of the value of the correlation coefficient, the *Langmuir* isotherm model is well fitted to the Th(IV) adsorption behavior on TTA-SBA-15 ( $R^2=1$ ). The high  $E$  value ( $40.82 \text{ kJ mol}^{-1}$ ) derived from the *D–R* isotherm model indicates that the particle diffusion mechanism plays an important role in the adsorption.

The temperature effect on Th(IV) adsorption was investigated within the range of 293–323 K. The experimental conditions were as follows: pH 4, initial concentration  $50 \text{ mg L}^{-1}$ , adsorbent amount 0.05 g, volume 25 mL, and contact time 30 min. The results of the experiment revealed that the temperature does not significantly affect Th(IV) adsorption. The average value of the results obtained was  $24.72 \pm 0.03 \text{ mg L}^{-1}$ . Additionally, the contact time effect on Th(IV) adsorption was performed within the range of 5–360 min. Temperature was kept at 293 K; however, the rest of the experimental conditions were the same as those for the testing of the temperature effect. Once again, no significant difference was found in the results. (Average result was  $24.80 \pm 0.04 \text{ mg L}^{-1}$ .) These insignificant effects of temperature and contact time between the mentioned ranges could be related to the strong chemical interaction between adsorbent and adsorbate. This deduction correlates with *D–R* isotherm results.

Modified and unmodified adsorbents were tested in identical conditions for control of adsorption efficiency. The experimental conditions for both SBA-15 and TTA-SBA-15 were set as follows: pH 4, initial concentration  $80 \text{ mg L}^{-1}$ , adsorbent amount 0.05 g, volume 25 mL, temperature 293 K, and contact time 30 min. The results of five parallel experiments show that on average the uptake

**Fig. 2** FT-IR spectra of SBA-15 (a) and TTA-SBA-15 (b)



of Th(IV) was  $19.6 \pm 0.6 \text{ mg g}^{-1}$  on SBA-15 and  $39.8 \pm 0.06 \text{ mg g}^{-1}$  on TTA-SBA-15. Thus, a significant increase in uptake capacity was shown to occur when the SBA-15 material was modified.

For comparison, other studies displaying the results of adsorption capacity and equilibrium are shown in Table 3. As seen from the results, the TTA-SBA-15 adsorbent shows highly rapid kinetic adsorption capacity. These fast adsorption kinetics are one of the advantages of the SBA-15 structure and give a favorable feature to the obtained material.

#### 3.2.4 Effect of coexisting ions on Th(IV) adsorption

To test the effect of coexisting ions on Th(IV) adsorption, an aqueous solution containing Th, U, Ca, Fe, and Mg ions was prepared, where the concentration of

each ion was set to  $80 \text{ mg L}^{-1}$ . Experiments were carried out as a function of pH to test the environment acidity of competing ions. The results of the experiments can be seen in Fig. 6. An increase in Th(IV) uptake by an increase in pH can be seen for both experiments. Nevertheless, the uptake of Th(IV) was reduced by 47.39% at pH 3 and 19.73% at pH 4 due to coexisting ions. This decrease is understandable because of the sharing of active sites on the adsorbent by thorium ions with coexisting ions. However, the decrease in Th(IV) uptake at pH 4 is less than that at pH 3. This can be explained by the different speciation of coexisting ions. The results reveal that Th(IV) adsorption was continuing even in the presence of competitive ions, despite a slight decrease in adsorption efficiency. As a conclusion, TTA-SBA-15 adsorbent has a potential use in the treatment of Th(IV) contaminated water.

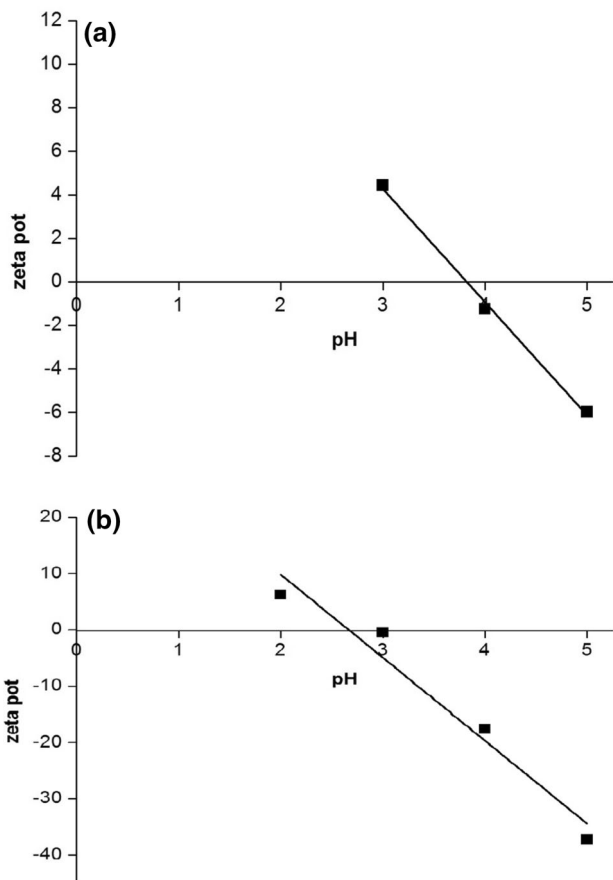


**Fig. 3** Zeta potential variations of SBA-15 (a) and TTA-SBA-15 (b), as a function of pH

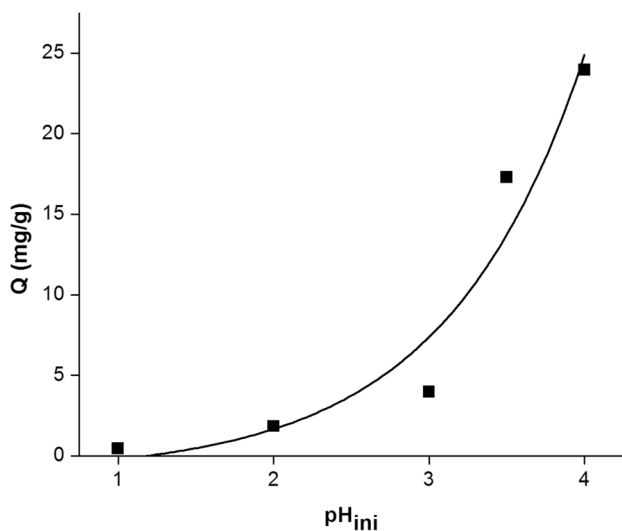


**Fig. 4** Effect of pH on the adsorption of Th(IV) by TTA-SBA-15 adsorbent (initial concentration:  $50 \text{ mg L}^{-1}$ , temperature:  $25 \text{ }^\circ\text{C}$ , contact time: 2 h, amount of sorbent: 0.05 g)

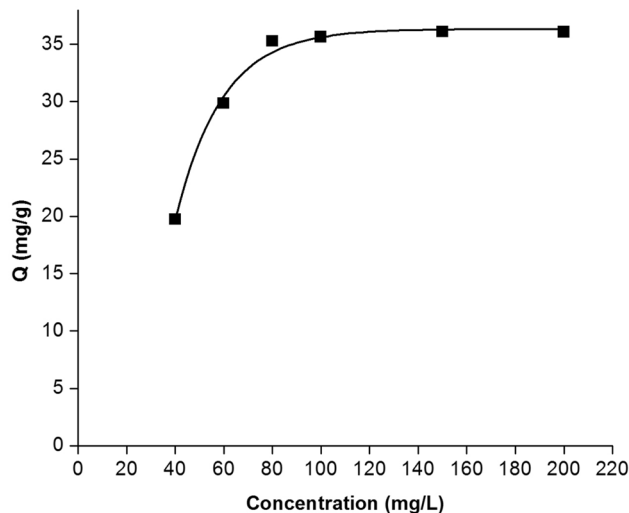


**Fig. 5** Effect of the initial metal concentration on the adsorption of Th(IV) by TTA-SBA-15 adsorbent ( $\text{pH}_{\text{ini}} 4$ , temperature:  $25 \text{ }^\circ\text{C}$ , contact time: 30 min, amount of sorbent: 0.05 g)

**Table 2** Langmuir, Freundlich, and *D-R* parameters for the adsorption of Th(IV) on TTA-SBA-15

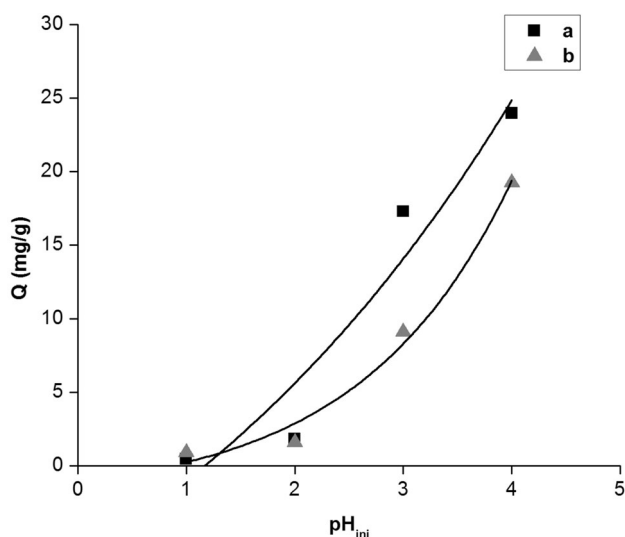
Isotherm models	Parameters	Values
<i>Langmuir</i>	$n_m \text{ (mg g}^{-1}\text{)}$	36.10
	$b \text{ (L mg}^{-1}\text{)}$	0.0002
	$R^2$	1
<i>Freundlich</i>	$n$	30.67
	$k \text{ (L mg}^{-1}\text{)}$	4.66
	$R^2$	0.90
<i>D-R</i>	$X_m \text{ (mmol g}^{-1}\text{)}$	0.17
	$E \text{ (kJ mol}^{-1}\text{)}$	40.82
	$R^2$	0.94

## 4 Conclusion

In this paper, we prepared thenoyltrifluoroacetone modified SBA-15 mesoporous silica structure for thorium adsorption. The increase in the adsorption of thorium was observed at an initial pH of 4. The uptake of Th(IV) reached a plateau after an initial concentration of  $100 \text{ mg L}^{-1}$ . The Langmuir isotherm model was found to be a suitable model for describing thorium adsorption onto TTA-SBA-15. The *Dubinin-Radushkevich* isotherm model revealed that a strong chemical interaction occurred between the adsorbent and the adsorbate. Temperature and contact time appeared to have no significant effect on the adsorption process within the range of experimental conditions. The results of the experiments indicate that TTA-SBA-15 is a very effective adsorbent in recovering Th(IV) from aqueous solutions, and could be a promising area of further development from an environmental and economical point of view.

**Table 3** Comparison of the adsorption properties between the presented method and other methods

Material	$Q$ uptake ( $\text{mg g}^{-1}$ )	Equilibrium time (min)	References
Modified clays	30.0	7.50	[37]
Modified mesoporous silica	49.0	3.00	[38]
Modified mesoporous silica	81.0	30.0	[39]
Mesoporous molecular sieves	214	720	[40]
Bifunctional groups modified mesoporous silica	164	60.0	[41]
Flux calcined diatomite	13.0	20.0	[42]
Activated carbon	21.0	30.0	[43]
This study	36.0	5.00	–

**Fig. 6** Variations of Th(IV) adsorption as a function of pH (with (b) and without (a) coexisting ions)

## References

- M.E. Nasab, S.A. Milani, A. Sam, Extractive separation of Th (IV), U(VI), Ti(IV), La(III) and Fe(III) from Zarigan ore. *J. Radioanal. Nucl. Chem.* **288**, 677–683 (2011). <https://doi.org/10.1007/s10967-011-1008-z>
- M.O.A. El-Magied, A.A. Tolba, H.S. El-Gendy et al., Studies on the recovery of Th(IV) ions from nitric acid solutions using amino-magnetic glycidyl methacrylate resins and application to granite leach liquors. *Hydrometallurgy* **169**, 89–98 (2017). <https://doi.org/10.1016/j.hydromet.2016.12.011>
- S.V. Bhat, J.S. Melo, B.B. Chaugule et al., Biosorption characteristics of uranium(VI) from aqueous medium onto *Catenella repens*, a red alga. *J. Hazard. Mater.* **158**, 628–635 (2008). <https://doi.org/10.1016/j.jhazmat.2008.02.042>
- W. Liu, X. Dai, Z. Bai et al., Highly sensitive and selective uranium detection in natural water systems using a luminescent mesoporous metal–organic framework equipped with abundant Lewis basic sites: a combined batch, X-ray absorption spectroscopy, and first principles simulation investigation. *Environ. Sci. Technol.* **51**, 3911–3921 (2017). <https://doi.org/10.1021/acs.est.6b06305>
- D. Sheng, L. Zhu, C. Xu et al., Efficient and selective uptake of  $\text{TcO}_4^-$  by a cationic metal–organic framework material with open  $\text{Ag}^+$  sites. *Environ. Sci. Technol.* **51**, 3471–3479 (2017). <https://doi.org/10.1021/acs.est.7b00339>
- T. Zheng, Z. Yang, D. Gui et al., Overcoming the crystallization and designability issues in the ultrastable zirconium phosphonate framework system. *Nat. Commun.* **8**, 15369 (2017). <https://doi.org/10.1038/ncomms15369>
- Y. Wang, Z. Liu, Y. Li et al., Umbellate distortions of the uranyl coordination environment result in a stable and porous polycatenated framework that can effectively remove cesium from aqueous solutions. *J. Am. Chem. Soc.* **137**, 6144–6147 (2015). <https://doi.org/10.1021/jacs.5b02480>
- D. Alipour, A.R. Keshtkar, M.A. Moosavian, Adsorption of thorium(IV) from simulated radioactive solutions using a novel electrospun PVA/TiO<sub>2</sub>/ZnO nanofiber adsorbent functionalized with mercapto groups: study in single and multi-component systems. *Appl. Surf. Sci.* **366**, 19–29 (2016). <https://doi.org/10.1016/j.apsusc.2016.01.049>
- L. Weijuan, T. Zuyi, Comparative study on Th(IV) sorption on alumina and silica from aqueous solutions. *J. Radioanal. Nucl. Chem.* **254**(1), 187–192 (2002). <https://doi.org/10.1023/A:1020874405480>
- L. Yan, F. Qiaohui, W. Wangsuo, Sorption of Th(IV) on goethite: effects of pH, ionic strength, FA and phosphate. *J. Radioanal. Nucl. Chem.* **289**, 865–871 (2011). <https://doi.org/10.1007/s10967-011-1166-z>
- G. Zhijun, N. Lijun, T. Zuyi, Sorption of Th(IV) ions onto TiO<sub>2</sub>: effects of contact time, ionic strength, thorium concentration and phosphate. *J. Radioanal. Nucl. Chem.* **266**(2), 333–338 (2005). <https://doi.org/10.1007/s10967-005-0912-5>
- M. Kruk, M. Jaroniec, A. Sayari, New insights into pore-size expansion of mesoporous silicates using long-chain amines. *Microporous Mesoporous Mater.* **35–36**, 545–553 (2000). [https://doi.org/10.1016/S1387-1811\(99\)00249-8](https://doi.org/10.1016/S1387-1811(99)00249-8)
- H. Yoshitake, Highly-controlled synthesis of organic layers on mesoporous silica: their structure and application to toxic ion adsorptions. *New J. Chem.* **29**, 1107–1117 (2005). <https://doi.org/10.1039/b504957a>
- D. Zhao, J. Feng, Q. Huo et al., Triblock copolymer syntheses of mesoporous silica with periodic 50–300 angstrom pores. *Science* **279**, 548–552 (1998). <https://doi.org/10.1126/science.279.5350.548>
- E. Da'na, Adsorption of heavy metals on functionalized-mesoporous silica: a review. *Microporous Mesoporous Mater.* **247**, 145–157 (2017). <https://doi.org/10.1016/j.micromeso.2017.03.050>

16. L. Dolatyari, M.R. Yaftian, S. Rostamnia, Removal of uranium (VI) ions from aqueous solutions using Schiff base functionalized SBA-15 mesoporous silica materials. *J. Environ. Manag.* **169**, 8–17 (2016). <https://doi.org/10.1016/j.jenvman.2015.12.005>
17. S. Wang, K. Wang, C. Dai et al., Adsorption of Pb<sup>2+</sup> on amino-functionalized core-shell magnetic mesoporous SBA-15 silica composite. *Chem. Eng. J.* **262**, 897–903 (2015). <https://doi.org/10.1016/j.cej.2014.10.035>
18. L. Giraldo, J.C.M. Piraján, Study on the adsorption of heavy metal ions from aqueous solution on modified SBA-15. *Mater. Res.* **16**(4), 745–754 (2013). <https://doi.org/10.1590/S1516-14392013005000051>
19. A. Shahbazi, H. Younesi, A. Badii, Batch and fixed-bed column adsorption of Cu(II), Pb(II) and Cd(II) from aqueous solution onto functionalised SBA-15 mesoporous silica. *Can. J. Chem. Eng.* **91**, 739–750 (2013). <https://doi.org/10.1002/cjce.21691>
20. G.R. Harvianto, S.H. Kim, C.S. Ju, Solvent extraction and stripping of lithium ion from aqueous solution and its application to seawater. *Rare Met.* **35**(12), 948–953 (2016). <https://doi.org/10.1007/s12598-015-0453-1>
21. D.R. Raut, P.K. Mohapatra, Extraction of uranyl ion using 2-thenoyltrifluoro acetone (HTTA) in room temperature ionic liquids. *Sep. Sci. Technol.* **50**, 380–386 (2015). <https://doi.org/10.1080/01496395.2014.973523>
22. Y. Li, B. Yan, Y. Li, Hybrid materials of SBA-16 functionalized by rare earth (Eu<sup>3+</sup>, Tb<sup>3+</sup>) complexes of modified  $\beta$ -diketone (TTA and DBM): covalently bonding assembly and photophysical properties. *J. Solid State Chem.* **183**(4), 871–877 (2010). <https://doi.org/10.1016/j.jssc.2010.02.006>
23. B. Yan, Y. Li, B. Zhou, Covalently bonding assembly and photophysical properties of luminescent hybrids Eu-TTA-Si and Eu-TTA-Si-MCM-41 by modified thenoyltrifluoroacetone. *Microporous Mesoporous Mater.* **120**, 317–324 (2009). <https://doi.org/10.1016/j.micromeso.2008.11.021>
24. J. Bassil, A. Al-Barazi, P. Da Costa et al., Catalytic combustion of methane over mesoporous silica supported palladium. *Catal. Today* **176**(1), 36–40 (2011). <https://doi.org/10.1016/j.cattod.2011.05.026>
25. J. Du, H. Xu, J. Shen et al., Catalytic dehydrogenation and cracking of industrial dipentene over M/SBA-15 (M=Al, Zn) catalysts. *Appl. Catal. A Gener.* **296**, 186–193 (2005). <https://doi.org/10.1016/j.apcata.2005.08.030>
26. E. Ghedini, F. Menegazzo, M. Signoretto et al., Mesoporous silica as support for Pd-catalyzed H<sub>2</sub>O<sub>2</sub> direct synthesis: effect of textural properties of the support on the activity and selectivity. *J. Catal.* **273**(2), 266–273 (2010). <https://doi.org/10.1016/j.jcat.2010.06.003>
27. P. Wang, Z. Wang, J. Li et al., Preparation, characterization and catalytic characteristics of Pd nanoparticles encapsulated in mesoporous silica. *Microporous Mesoporous Mater.* **116**(1), 400–405 (2008). <https://doi.org/10.1016/j.micromeso.2008.04.029>
28. A.M. Venezia, G. Di Carlo, L.F. Liotta et al., Effect of Ti(IV) loading CH<sub>4</sub> oxidation activity and SO<sub>2</sub> tolerance of Pd catalysts supported on silica SBA-15 and HMS. *Appl. Catal. B Environ.* **106**, 529–539 (2011). <https://doi.org/10.1016/j.apcatb.2011.06.013>
29. F. Yin, S. Ji, P. Wu et al., Deactivation behavior of Pd-based SBA-15 mesoporous silica for the catalytic combustion of methane. *J. Catal.* **257**(1), 108–116 (2008). <https://doi.org/10.1016/j.jcat.2008.04.010>
30. S.B. Sarrin, Analytical use of arsenazo III: determination of thorium, zirconium, uranium and rare earth elements. *Talanta* **8**, 673–685 (1961). [https://doi.org/10.1016/0039-9140\(61\)80164-1](https://doi.org/10.1016/0039-9140(61)80164-1)
31. L. Cromières, V. Moulin, B. Fourest et al., Sorption of thorium onto hematite colloids. *Radiochim. Acta* **82**, 249–256 (1998). <https://doi.org/10.1524/ract.1998.82.special-issue.249>
32. P. Sar, S.F. D'Souza, Biosorption of thorium (IV) by a *Pseudomonas* biomass. *Biotechnol. Lett.* **24**, 239–243 (2002). <https://doi.org/10.1023/A:1014153913287>
33. Ş. Sert, C. Kütahyalı, S. İnan et al., Biosorption of lanthanum and cerium from aqueous solutions by *Platanus orientalis* leaf powder. *Hydrometallurgy* **90**, 13–18 (2008). <https://doi.org/10.1016/j.hydromet.2007.09.006>
34. S. Sert, M. Eral, Uranium adsorption studies on aminopropyl modified mesoporous sorbent (NH<sub>2</sub>-MCM-41) using statistical design method. *J. Nucl. Mater.* **406**, 285–292 (2010). <https://doi.org/10.1016/j.jnucmat.2010.08.024>
35. S. Yusan, S. Akyil, Sorption of uranium(VI) from aqueous solutions by akaganeite. *J. Hazard. Mater.* **160**, 388–395 (2008). <https://doi.org/10.1016/j.jhazmat.2008.03.009>
36. H.K. Boparai, M. Joseph, D.M. O'Carroll, Kinetics and thermodynamics of cadmium ion removal by adsorption onto nano zerovalent iron particles. *J. Hazard. Mater.* **186**, 458–465 (2011). <https://doi.org/10.1016/j.jhazmat.2010.11.029>
37. D.L. Guerraa, R.R. Viana, C. Airoidi, Adsorption of thorium cation on modified clays MTTZ derivative. *J. Hazard. Mater.* **168**, 1504–1511 (2009). <https://doi.org/10.1016/j.jhazmat.2009.03.034>
38. S.R. Yousefi, S.J. Ahmadi, F. Shemirania et al., Simultaneous extraction and preconcentration of uranium and thorium in aqueous samples by new modified mesoporous silica prior to inductively coupled plasma optical emission spectrometry determination. *Talanta* **80**, 212–217 (2009). <https://doi.org/10.1016/j.talanta.2009.06.058>
39. L. Dolatyari, M.R. Yaftian, S. Rostamnia, Adsorption characteristics of Eu(III) and Th(IV) ions onto modified mesoporous silica SBA-15 materials. *J. Taiwan Inst. Chem. Eng.* **60**, 174–184 (2016). <https://doi.org/10.1016/j.jtice.2015.11.004>
40. L. Zuo, S. Yu, H. Zhou et al., Th(IV) adsorption on mesoporous molecular sieves: effects of contact time, solid content, pH, ionic strength, foreign ions and temperature. *J. Radioanal. Nucl. Chem.* **288**, 379–387 (2011). <https://doi.org/10.1007/s10967-010-0930-9>
41. L.Y. Yuan, Z.Q. Bai, R. Zhao et al., Introduction of bifunctional groups into mesoporous silica for enhancing uptake of thorium (IV) from aqueous solution. *Appl. Mater. Interfaces* **6**, 4786–4796 (2014). <https://doi.org/10.1021/am405584h>
42. S. Yusan, C. Gok, S. Erenturk et al., Adsorptive removal of thorium (IV) using calcined and flux calcined diatomite from Turkey: evaluation of equilibrium, kinetic and thermodynamic data. *Appl. Clay Sci.* **67–68**, 106–116 (2012). <https://doi.org/10.1016/j.clay.2012.05.012>
43. C. Kütahyalı, M. Eral, Sorption studies of uranium and thorium on activated carbon prepared from olive stones: kinetic and thermodynamic aspects. *J. Nucl. Mater.* **396**, 251–256 (2010). <https://doi.org/10.1016/j.jnucmat.2009.11.018>